

## Research Article

# Contribution of the Residual Body in the Spatial Organization of *Toxoplasma gondii* Tachyzoites within the Parasitophorous Vacuole

S. Muñiz-Hernández,<sup>1,2</sup> M. González del Carmen,<sup>1,3</sup> M. Mondragón,<sup>1</sup> C. Mercier,<sup>3</sup> M. F. Cesbron,<sup>4,5</sup> S. L. Mondragón-González,<sup>6</sup> S. González,<sup>7</sup> and R. Mondragón<sup>1</sup>

<sup>1</sup>Departamento de Bioquímica, Centro de Investigación y de Estudios Avanzados del Instituto Politécnico Nacional (CINVESTAV-IPN), Avenue IPN No 2508, San Pedro Zacatenco, Gustavo A. Madero 07360 Mexico City, Mexico

<sup>2</sup>Subdirección de Investigación Básica, Instituto Nacional de Cancerología, Secretaría de Salud, 14080 Mexico City, Mexico

<sup>3</sup>Facultad de Medicina, Universidad Veracruzana, Avenue Hidalgo, Esq. Carrillo Puerto s/n, Col. Centro, 94740, VER, Mexico

<sup>4</sup>Laboratoire Adaptation et Pathogénie des Microorganismes, Université Joseph Fourier Grenoble 1, BP 170, 38042 Grenoble Cedex 9, France

<sup>5</sup>Center National de la Recherche Scientifique, UMR 5163, BP 170, 38042 Grenoble Cedex 9, France

<sup>6</sup>Unidad Profesional Interdisciplinaria en Ingeniería y Tecnologías Avanzadas, IPN, Avenue IPN 2580, Gustavo A. Madero 7340 Mexico City, Mexico

<sup>7</sup>Unidad de Microscopía Electrónica, CINVESTAV-IPN, Mexico

Correspondence should be addressed to R. Mondragón, ricardo\_mflores@hotmail.com

Received 4 July 2011; Revised 29 August 2011; Accepted 31 August 2011

Academic Editor: Jorge Morales-Montor

Copyright © 2011 S. Muñiz-Hernández et al. This is an open access article distributed under the Creative Commons Attribution License, which permits unrestricted use, distribution, and reproduction in any medium, provided the original work is properly cited.

*Toxoplasma gondii* proliferates and organizes within a parasitophorous vacuole in rosettes around a residual body and is surrounded by a membranous nanotubular network whose function remains unclear. Here, we characterized structure and function of the residual body in intracellular tachyzoites of the RH strain. Our data showed the residual body as a body limited by a membrane formed during proliferation of tachyzoites probably through the secretion of components and a pinching event of the membrane at the posterior end. It contributes in the intravacuolar parasite organization by the membrane connection between the tachyzoites posterior end and the residual body membrane to give place to the rosette conformation. Radial distribution of parasites in rosettes favors an efficient exteriorization. Absence of the network and presence of atypical residual bodies in a  $\Delta$ GRA2-HXGPRT knock-out mutant affected the intravacuolar organization of tachyzoites and their exteriorization.

## 1. Introduction

*Toxoplasma gondii* is an obligate intracellular parasite that actively invades host cells through a sequential secretion of proteins from Apicomplexa-specific secretory organelles, namely, micronemes and rhoptries [1] as well as by the participation of the parasite motility based on its subpellicular cytoskeleton [2]. The highly replicative and invasive form of *Toxoplasma*, the tachyzoite, proliferates within an intracellular compartment named the parasitophorous vacuole (PV). The PV delimiting membrane (PVM) is formed at the time of invasion from both the host cell membrane components and

parasite-secreted products [3, 4]. Once installed within the host cell, the PV is rapidly engaged by host cell intermediate filaments and microtubules [5], whilst the PVM associates with host cell mitochondria and endoplasmic reticulum [6–8]. Studies showed the formation of host-microtubules-based invaginations of the PVM—named Host Sequestering Tubulo-structures or HOSTs [5]—that serve as conduits for nutrient acquisition from the host cytoplasm to the PV lumen. Apart from rhoptry proteins [9], the PVM is also decorated with several proteins secreted from a third type of Apicomplexa-specific secretory organelles, the dense granules, which contain the GRA proteins [1].

Observation of infected cells by electron microscopy showed that a membranous nanotubular network (MNN) of 40–60 nm in diameter assembles at the invaginated posterior end of the parasite during the first hour following invasion and further extends into the PV space in order to connect with the PVM [10]. Immunoelectron microscopy analysis showed that the MNN has a stable association with several GRA proteins including GRA2 [10], GRA4 [11], GRA6 [11], and GRA9 [12] and showed that GRA2 contributes to the formation of a multiprotein complex within the MNN [13]. Transmission electron microscopy (TEM) analysis in thin sections of embedded infected host cells with GRA2 *Toxoplasma* knock-out mutant showed that deletion of the corresponding gene leads to complete disappearance of the MNN without altering parasite *in vitro* proliferation [14, 15].

Once tachyzoites have established metabolic connections with the host cell by means of the MNN, the HOSTS, and the PVM, they begin to divide asexually mainly by endodiogeny, a process that is characterized by the synchronous assembling of two daughter parasites within each mother cell. Once two sets of intracellular organelles have been assembled within the mother cell, daughter cells emerge from the mother, leaving remnants of the mother cell at their posterior end [16]. These apparent remnants have been referred to as the residual body (RB) of division [17]. After the third division, tachyzoites organize in rosettes around the RB. To date there is not data about the fine structure of the RB or its function.

Analysis of the intravacuolar arrangement of tachyzoites during endodiogeny has been successfully achieved by transmission electron microscopy (TEM) [15, 18, 19]. By using a method proposed by Tanaka for scanning electron microscopy (SEM) in which apical plasma membrane is removed thus preserving the integrity and spatial distribution of intracellular compartments and organelles [15, 18, 19], it was possible to know the relationship between the intravacuolar organization of proliferating tachyzoites and the MMN [15, 18, 19].

In the present study we characterized the intravacuolar organization of tachyzoites of the RH strain of *T. gondii* in rosettes during proliferation in an attempt to better characterize origin, structure, and function of the RB. We additionally determined the contribution of GRA2 protein in the intravacuolar organization of tachyzoites by studying GRA2 knock-out mutant-infected cells.

## 2. Materials and Methods

All reagents were purchased from SIGMA (St Louis, Mo). Specific reagents for electron microscopy were from Polysciences (Warrington, Pa) unless otherwise indicated.

**2.1. Animals.** BALB/c mice used for parasite infections were maintained in an animal facility with regulated environmental conditions in terms of temperature, humidity, and filtered air. Animals were maintained according to the country official norm NOM-062-ZOO-1999 (<http://www.sagarpa.gob.mx/Dgg/NOM/062zoo.pdf>) for the production, care, and use of laboratory animals (México).

**2.2. Cell Culture and Preparation of Parasites.** Madin-Darby Canine Kidney epithelial cells (MDCK, ATCC-CCL 34) were used as host cells for both parasite invasion and proliferation. MDCK cells were maintained in Dulbecco Minimum Essential Medium (DMEM) (GIBCO, USA), supplemented with 10% fetal calf serum (FCS, Equitech-Bio, USA), under a 5% CO<sub>2</sub> atmosphere, at 37°C.

Parasites of the RH strain (wild type) were maintained by intraperitoneal passages in female Balb/c mice [20]. After cervical dislocation, tachyzoites were harvested from intraperitoneal exudates, washed in phosphate-buffered saline (PBS, 138 mM NaCl, 2.7 mM KCl, 8.1 mM Na<sub>2</sub>HPO<sub>4</sub>, 1.1 mM KH<sub>2</sub>PO<sub>4</sub>, and pH 7.4), and filtered through 3 μm pore polycarbonate membranes (Millipore, Bedford, Mass) [20].

The ΔGRA2-HXGPRT knock-out mutant [15] constructed in the RH strain background and was maintained in MDCK cells. Prior to each experiment, cells were lysed and parasites were harvested, rinsed in PBS, counted, and suspended in appropriate medium.

**2.3. Infection of MDCK Cells with Tachyzoites.** MDCK host cells were grown on sterile coverslips in DMEM supplemented with 10% FCS for 24 h to reach between 80–90% confluency. Cells were exposed to parasites at the ratio of 5 : 1 parasites per host cell, incubated for 2 h and washed with PBS to discard extracellular parasites. Infected MDCK cells were maintained in DMEM with 10% fetal calf serum under a 5% CO<sub>2</sub> atmosphere at 37°C and at desired times.

**2.4. Identification of Components of RB by Immunofluorescence.** MDCK cells infected for 24 h were fixed in 3.7% paraformaldehyde for 20 min, permeabilized for 10 min in 0.1% Triton X-100, blocked in 0.5% BSA, and incubated for 2 h with the following primary antibodies diluted in PBS: monoclonal antibody (mAb) TG05.54 anti-SAG1 [21], mAb TG17.43 anti-GRA1, mAb TG17.179 anti-GRA2 [22], and rabbit serum anti-GRA6 [11], each at the dilution of 1 : 500, or mAb T5.2A3 anti-ROP1, mAb T34A5 anti-ROP2, each at the dilution of 1 : 25 [23] (the mAbs anti-ROP proteins were provided by J. F. Dubremetz, CNRS UMR 5539, Université Montpellier II, France, and the rabbit serum anti-GRA6 was obtained from L. D. Sibley, Department of Molecular Microbiology, Washington School of Medicine, Saint-Louis, MO). Cells were rinsed in PBS, incubated for 1 h with goat anti-mouse IgG (H+L) or with goat anti-rabbit IgG (H+L), both coupled to Alexa Fluor 488 (Molecular Probes, USA). To detect nuclei in tachyzoites organized in rosettes, cells were incubated for 1 h with 10 μg/mL of the fluorescent stain 4'6-diamidino-2-phenylindole specific for double-stranded DNA (DAPI, Sigma-Aldrich Co., Mexico).

Coverslips were mounted on glass slides in Vectashield Mounting Medium (Vector Laboratories, UK) and analyzed with an AxioScope II fluorescence microscope coupled to an AxioCam II RC digital camera (Carl Zeiss). Fluorescent images were acquired and processed using the AxioVision software 4.5.

**2.5. Fine Structure of the RB by TEM and SEM-Tanaka.** For TEM, MDCK cells infected for 24 h were fixed for 1 h in 2.5%

glutaraldehyde. Cell monolayers were scraped off, rinsed in PBS and fixed for 1 h in 1% OsO<sub>4</sub> at 4°C, rinsed, gradually dehydrated in ethanol, and finally embedded in Spurr's resin [20]. Thin sections were obtained with an Ultracut E ultramicrotome (Reichert Jung, Austria) and stained with uranyl acetate and lead citrate. Copper grids with the sections were examined in a JEOL 1400 transmission electron microscope at 80 keV (JEOL LTD, Japan). Digital images were obtained and processed with Adobe Photoshop software (USA).

For SEM using the Tanaka method, MDCK cells were infected for 1, 6, 12, and 24 h and then processed according to Travier et al. [15]. Briefly, at selected times, infected monolayers were fixed with 2% glutaraldehyde and 1% OsO<sub>4</sub> in PBS, ethanol dehydrated, critical point dried in CO<sub>2</sub> atmosphere in a Samdry-780A apparatus (Tousimis Research, USA), and gold coated in a Denton Vacuum Desk II (INXS, Inc, Florida) [20]. Coverslips containing the infected monolayers were attached to SEM aluminum holders, and the apical plasma membrane of host cells was removed by an adhesive tape. Both the treated coverslips and the adhesive tapes recovered from the rod were gold coated and analyzed using a SEM JEOL 65LV (JEOL, LTD, Japan). Digital images were recorded, and photocompositions were realized with the Adobe Photoshop software.

**2.6. Ionomycin-Induced Egress Assay.** Coverslips with MDCK cells infected for 24 h were mounted within observation chambers and then were exposed to 0.1 μM ionomycin (in 0.001% DMSO in PBS) to induce parasite egress [24]. Exteriorization was recorded under time lapse mode in a phase contrast microscope using an AxioCam RC digital camera (Carl Zeiss) and the AxioVision software. Sequential images were processed using the Adobe Photoshop software.

**2.7. Three-Dimensional Reconstruction of the Rosette.** Three-dimensional model of a rosette was built using AutoCAD software version 2007, and it was based on the morphological properties of intravacuolar tachyzoites micrographed by SEM and on the spatial distribution of the tachyzoites nuclei stained with the DAPI dye. Two orthogonal views were required to design the pictorial 3D rosette. The front isometric view of the tachyzoite, providing the width and height dimensions, was divided in 26 longitudinal sections of 190 nm, each with a total length of 5.14 μm. The top isometric view provided the width and depth dimensions of each cross-section. Both parameters were taken in consideration to create the geometry of the parasite, consisting of 26 planar section curves. Sweeping the planar sections along a defined spine designed to be the main geometry axis, allowed the creation of a complex multisection solid. Each 3D tachyzoite was adapted in specific position, around a 3D RB model, according to the interparasite distance observed in SEM micrographs of rosettes in order to construct the respective 3D digital model.

**2.8. Statistical Analysis.** Variance analysis of data was achieved by using the Student's *t*-test.

### 3. Results

**3.1. Tachyzoites Organize around an RB to Form Intravacuolar Rosettes.** By detaching the plasma membrane of infected cells, the spatial distribution of the intravacuolar tachyzoites was exposed further showing their relationship with the MNN and the RB under the high resolution of an SEM (Figure 1(b)). After 24 hours of proliferation, most of the tachyzoites were organized within the vacuole in rosettes around an RB located in the center of the structure (Figures 1(a) and 1(b), arrow). Tachyzoites were surrounded by the MNN and tightly associated through their posterior end to the RB (Figure 1(b)). During the detaching process, most of MNN and vacuolar components remained associated to the rosette while detached apical membrane remained free of parasites or of any MNN component (Figure 1(c)).

**3.2. The Residual Body Is Related to the Rosette Organization.** In SEM images, the RB was clearly identified as a round structure located in the center of the rosette with diameter of  $1.43 \mu\text{m} \pm 1.0$  (measured in 11 rosettes analyzed) that was linked to the posterior ends of parasites in proliferation (Figure 2(A), rectangle). A magnification of the interaction zone between the RB and the posterior end of the tachyzoites showed a close association between both membrane areas (Figure 2(B)). In order to further examine the fine structure of the RB and its relationship with the daughter tachyzoites in the rosette, thin sections of infected MDCK cells were analyzed by TEM. A membrane was found limiting the periphery of the RB (Figure 2(C), insets (a), (b)). At the interior of the RB were identified several organelles characteristics of tachyzoites such as dense granules, rhoptries, nuclear fragments, mitochondria, and Golgi between others, suggesting their origin from components that were trapped in the RB during the division of the tachyzoites (Figure 2(C)). The structural analysis of the interaction zone showed a membrane continuity between the membrane of the posterior end of the tachyzoites and the RB membrane, with the presence of an apparent communication between the cytoplasm of both the RB and the tachyzoites (Figures 2(C)–2(E), white arrows). In regions of the RB membrane not involved in the intermembrane interaction, we detected a typical three-membrane pellicle (Figure 2(C); inset (b)). According to the magnification shown in Figure 2(E), the polar posterior ring (indicated by double arrows) appears to contribute to stabilizing the intermembrane junction. Polar posterior ring of tachyzoites can be clearly identified by a submembrane electron dense zone at the posterior end of the tachyzoites.

Identification of some proteins present in the RB was made by immunofluorescence with antibodies against proteins from secretory organelles such as dense granules and rhoptries. Dense granule proteins GRA1, GRA2, and GRA6 that are normally secreted in the PV [1] were detected in the RB (Figure 3, arrows). Interestingly, GRA5, a protein that has been described associated with the PVM [22, 25], was also found in the RB. During the focusing of the tachyzoites in the rosettes by phase contrast microscopy, the definition of the RB was lost showing an apparent absence of the structure. When the RB is focused, then the rosette appeared blurry.

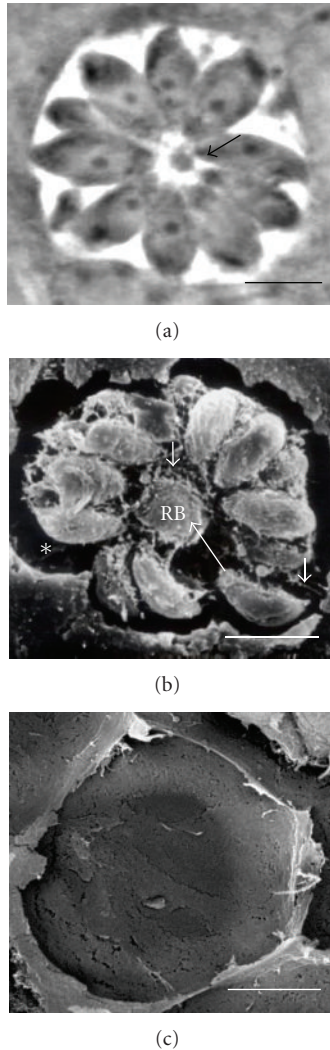


FIGURE 1: Intravacuolar organization of tachyzoites in MDCK cells. (a) Phase contrast micrograph of a rosette of intravacuolar tachyzoites and (b) SEM-Tanaka micrographs of a rosette (B). Long arrows indicate the RB; arrowheads show intravacuolar network extensions connecting parasites to the PVM; short arrows indicate the position of the apical end in tachyzoites; asterisks show the empty space observed around parasites, at the periphery of the PV. The counterpart of the PV was devoid of any material from the MNN or of tachyzoites (c). Bar = 5  $\mu$ m.

That is why we decided to focus on the rosette rather than the RB.

Antibodies against SAG1, the parasite major surface protein [21], labelled the plasma membrane of proliferating parasites but not the RB membrane (Figure 3, arrow in SAG1); probably the availability of the RB membrane was limited by the binding of the tachyzoites. Proteins from rhoptries ROP1 and ROP2 were detected only in the apical end of parasites but not in the RB indicating the specificity of the staining (Figure 3). DNA staining with DAPI showed the presence of the nuclei of tachyzoites and only a slight RB labeling (Figure 3). In the particular case of DAPI, we had to focus on the RB because the signal we were looking

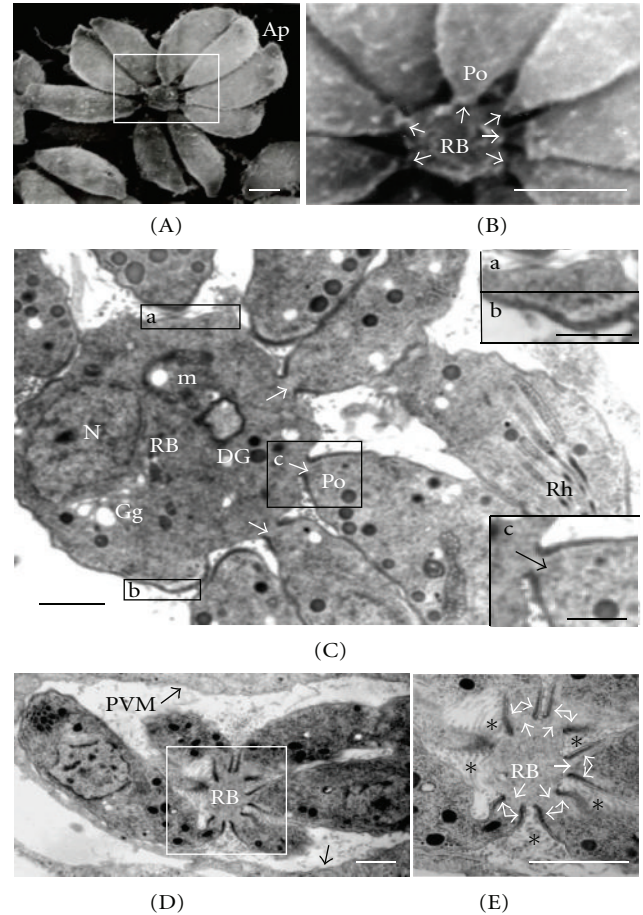


FIGURE 2: The residual body is a structure derived from a mother cell that contributes to the intravacuolar organization of parasites in rosettes. (A) Intravacuolar "rosette" micrographed after SEM-Tanaka processing. (B) Magnification of the area squared in (A) showing a link between the RB and the posterior ends of the proliferating tachyzoites (arrows). (C–E) micrographs obtained by thin sectioning. Arrows in (C–E) indicate membrane fusion between the RB limiting membrane and the tachyzoites membrane at the posterior end and the continuity between tachyzoites and the RB cytoplasm. (E) High magnification of the area squared in (D). Asterisks in (E) indicate accumulation of MNN at the periphery of the RB, and double arrows indicate parasites' posterior polar ring. Insets in (C) represent the different types of membranes that limit the RB: a unit membrane (a) or a pellicle-like composed of three layers (b). Inset (c) in (C) indicates membrane fusion between the RB and the posterior end of a parasite. Ap: apical end of the tachyzoite; DG: dense granule; Gg: Golgi; m: mitochondria; N: nucleus; PVM: parasitophorous vacuole membrane; Po: posterior end of the tachyzoite; RB: residual body; Rh: rhoptries. Bars = 1  $\mu$ m; Bars in insets b and c = 500 nm.

for was precisely within the RB, that is why in the image of phase contrast microscopy the RB appeared as a clear and well-defined structure.

**3.3. Formation of the RB and MNN during Intravacuolar Proliferation.** In order to characterize the formation of the RB during endodiogeny, infected MDCK cells were cultured

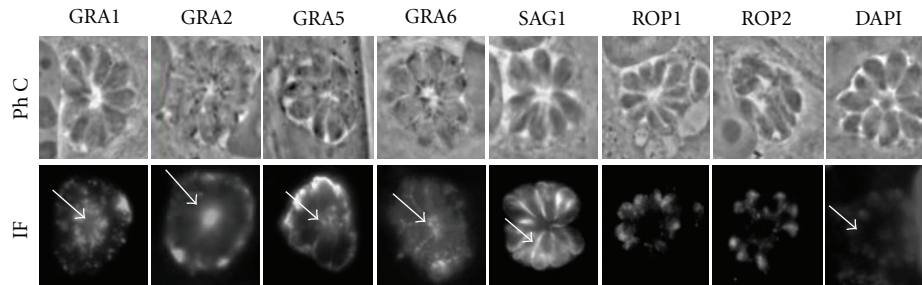


FIGURE 3: Localization of GRA proteins in the RB. MDCK cells infected with RH tachyzoites were incubated with antibodies directed against the dense granule proteins GRA1, GRA2, GRA5, and GRA6, rhoptry proteins (ROP1, 2), or membrane protein SAG1. GRA proteins marked the RB (arrows), while the stain with nuclear marker, DAPI, showed a weak staining of RB. Immunofluorescence micrographs (IF) are shown with their respective phase contrast microscopy images (PhC).

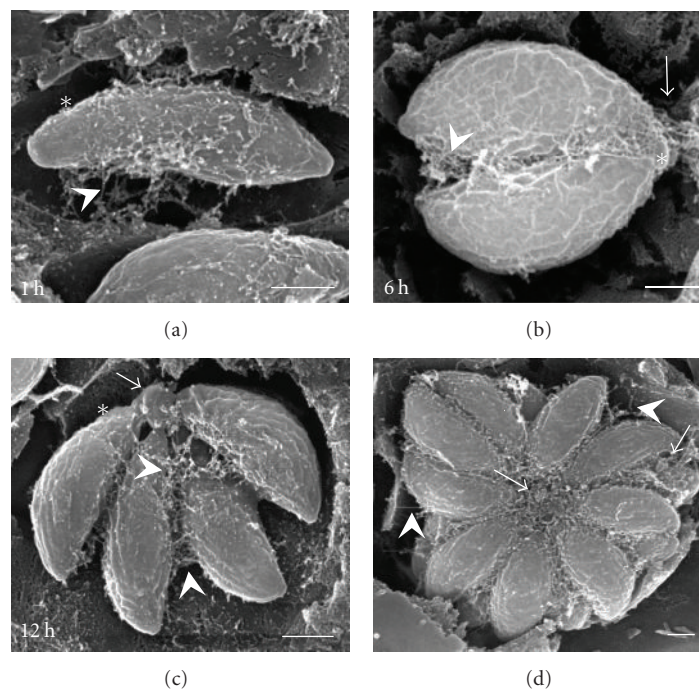


FIGURE 4: SEM-Tanaka sequence of intravacuolar proliferation of tachyzoites. Arrowheads indicate extensions of the MNN, which connect the incurved face of a single parasite to the PVM (1 h), the incurved faces of parasites after the first and second divisions (6, 12 h), or which connect the rosette to the PVM (24 h). Arrows point out the RB (6–24 h). Asterisks indicate the apparent empty space at the PV periphery (1–24 h). Timing indicated in lower left corners represents the replication time after invasion. Bars = 1  $\mu$ m.

for 1, 6, 12, and 24 h to obtain PVs containing 1, 2, 4, 8, and 16 parasites, and they were processed for SEM as described above. After 1 h of invasion, the MNN was detected mainly concentrated on the incurved face of recently invaded parasites (Figure 4(a)), forming a web that kept the first parasite attached to the PVM (arrowhead). Parasites that resulted from the first division at 6 h after invasion (Figure 4(b)) remained connected with the PVM via extensions of the MNN located at the parasite posterior ends (arrow) as well as on their incurved face (arrowhead). In addition, we detected a residual body that kept the two parasites united by their posterior ends (asterisk). At twelve hours after invasion, the RB acquired a spherical shape while the network that surrounded the parasites favoured interparasitic cohesion

(Figure 4(c)). At 24 h of proliferation of parasites, the RB was found in the centroid of the rosette with the presence of several parasitic interconnections (Figure 4(d), arrow). There were also connections between parasites and the PVM (arrowheads).

**3.4. The Residual Body Contributes to the Intravacuolar Organization of the Parasites.** To study whether the RB contributes to the efficient use of intravacuolar space by the proliferating parasites, tachyzoites organized in rosettes were stained with the fluorescent dye for nuclei, DAPI, and serial optical sections obtained in a confocal microscope (Figure 5(a)). Serial images showed that the nuclei and thus parasites are arranged in two adjacent planes which contain

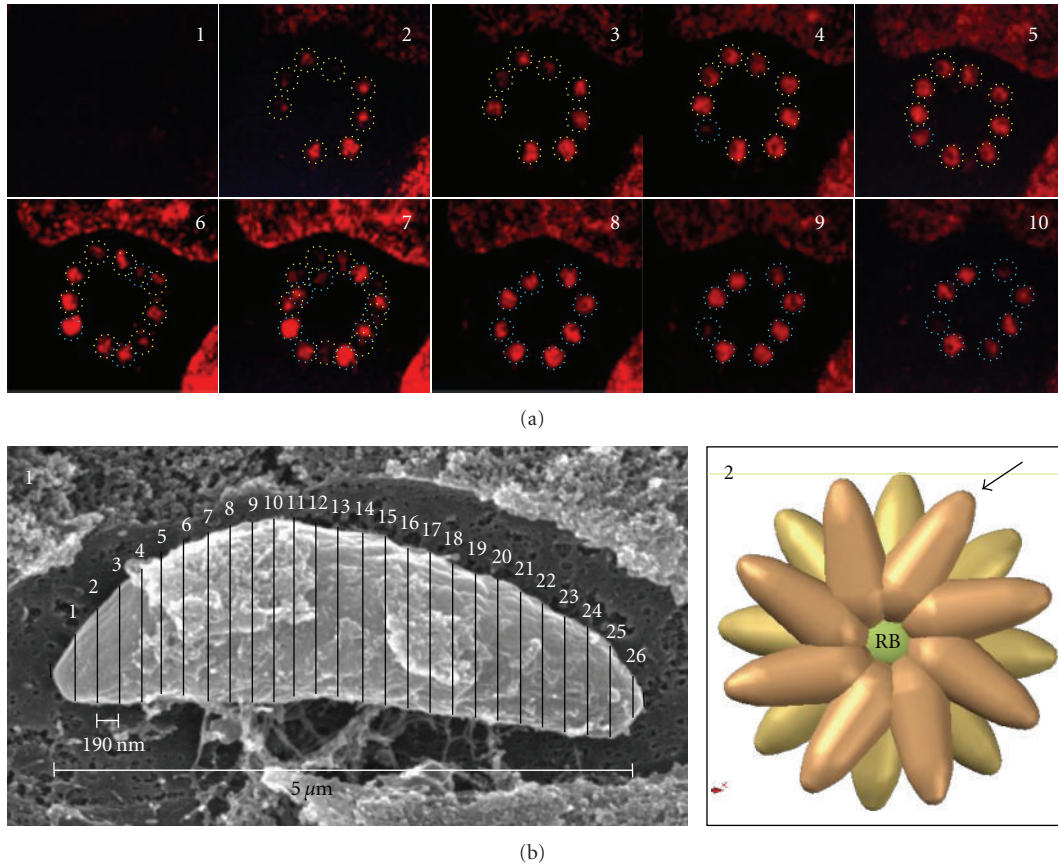


FIGURE 5: Proliferating tachyzoites arranged in rosettes are localized in two planes within the PV. (a) Confocal serial sections of proliferating tachyzoites arranged in rosette and stained with DAPI to show nuclear distribution. Confocal images 3 and 8 show the spatial arrangement of tachyzoites in two planes each containing 8 parasites. The interaction between both planes is showed in confocal image 7. (b) SEM-Tanaka micrograph of tachyzoite after 1 h of invasion that was used as a template to build the 3D digital model of the rosette; it was sectioned in 26 portions of 190 nm each and was used to build a digital model that was in turn used to design a 3D digital model of a rosette (C). Arrow, apical extreme of parasite, RB: residual body. Bar = 5  $\mu\text{m}$ .

each 8 parasites (Figure 5(a), insets 3 and 8 resp.). Parasites in both planes showed an interspersed distribution; however, in a certain optical section (inset 7) all nuclei were visible although with clear differences in their respective confocal planes (see inset 7, Figure 5(a)). By imaging tachyzoites and rosettes by SEM and their nuclei by confocal microscopy, we could develop a three-dimensional digital model of the rosette (Figures 1 and 5(b), and inset 1). The exact location of the parasites in the two planes was deduced from the images of the nuclei obtained by confocal microscopy (Figure 5(a)), resulting in the three-dimensional arrangement of the rosette shown in Figure 5(b) (inset 2). According to the 3D model of the rosette, the parasites are interspersed at different levels in order to optimize the available space. Each parasite is pointing outward in an organization in the form of wagon wheel in order to define possible externalization individual routes.

**3.5. The Absence of the MNN Alters the Cohesion between the Parasites and the Intravacuolar Arrangement.** The  $\Delta\text{GRA2-HXGPRT}$  strain ( $\Delta\text{GRA2}$ ) is an RH mutant knocked out for expression of GRA2 that has been previously characterized to lack of the typical MNN [14, 15]. We used the  $\Delta\text{GRA2}$

strain in order to determine if the lack of expression of GRA2 protein could modify the intravacuolar organization of the tachyzoites and the structure of the RB. Firstly, the absence of protein GRA2 did not alter the invasive capacity finding that approximately 40% of the cells were infected with both the RH strain as the  $\Delta\text{GRA2}$  strain (data not shown). To follow the intravacuolar development of the tachyzoites, cells were invaded for 1, 6, 12 and 24 h and processed for SEM as described in Figure 4. In all the intravacuolar development stages, tachyzoites were covered by an amorphous material (Figure 6). Typical RBs were not detected, and the MNN was observed as an abundant amorphous material covering the parasites with only few fibers interconnecting parasites and attaching them to the PVM (Figures 7(a) and 7(b), arrow-head). An interesting observation was to find  $\Delta\text{GRA2}$  strain at 24 h organized in clusters of 2 to 8 parasites in the same PV but not in the typical rosette arrangement (Figures 6(e) and 6(f), and 7). In most cases, a clear lack of interparasite cohesion was evidenced by the parasites separation even in the cluster distribution (E). Parasites were found attached to the RB through fibrous tubules leaving spacing between the body and the posterior end (Figures 6(e) and 6(f)). It

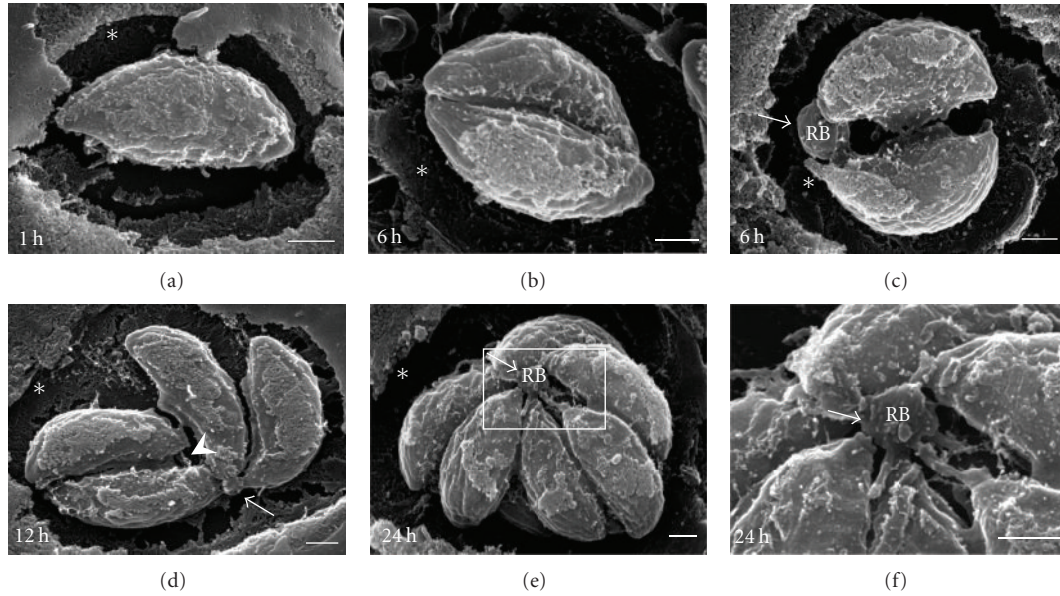


FIGURE 6: The intravacuolar MNN plays a structural role in keeping parasites tightly organized as “rosettes” during endodiogeny. (a–f) SEM-Tanaka micrographs of MDCK cells, infected by  $\Delta$ GRA2 mutant for 1, 6, 12, and 24 h, show loss of the MNN and alteration of interparasite cohesion within the PV. Arrows in (c–f) indicate residual amorphous and fibrous material at the parasites posterior end instead of the typical RB. Arrowheads in (d) show membranous fibers linking parasites together and to the PVM. Asterisks in (a–f) indicate an apparent empty space at the PV’s periphery. Bar = 1  $\mu$ m.

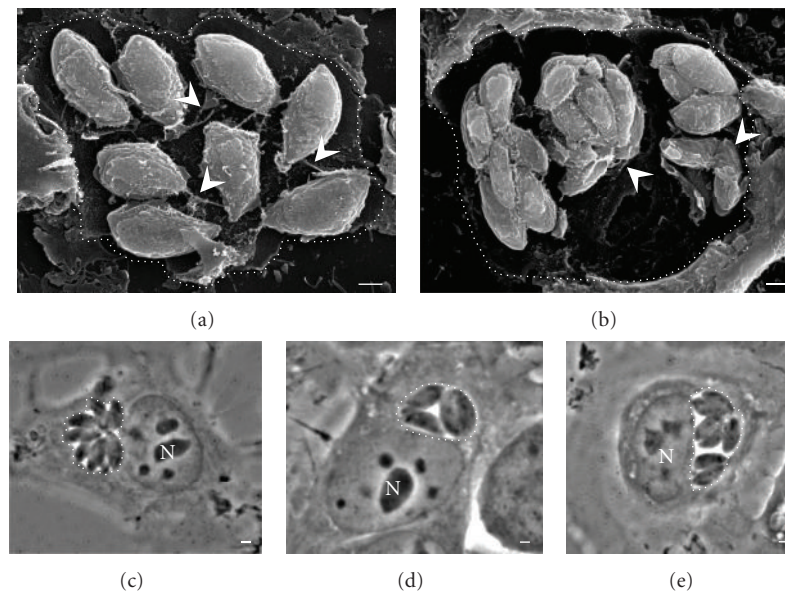


FIGURE 7: Absence of the GRA2 protein results in asynchrony of proliferation with loss of MNN, RB, and intravacuolar parasite cohesion. SEM-Tanaka micrographs of MDCK cells, infected by  $\Delta$ GRA2 mutants for 24 h, show loss of interparasite cohesion with presence of isolated parasite aggregates within the same PV (a, b). Arrowheads indicate membranous fibers cross-linking parasites and parasites connected to the PVM. Phase contrast micrographs of live MDCK cells infected with (c) RH *Toxoplasma* strain or (d, e)  $\Delta$ GRA2 parasites. Dotted lines were drawn to delimit the PVs. Bars = 1  $\mu$ m.

is possible that the structural modifications of the RB and the type of interaction with the tachyzoites altered somehow the intravacuolar organization, therefore rosettes were not formed.

**3.6. The RB Promotes an Orderly and Efficient Externalization of the Parasites.** To determine the involvement of RB in the

externalization of the tachyzoites from infected cells, MDCK cells infected with RH or  $\Delta$ GRA2 strains were exposed to calcium ionophore ionomycin to induce the externalization, and this was recorded in real time by time-lapse video microscopy. Parasites of the RH strain left the PV and the host cell after the ionomycin stimulus by propelling themselves in a synchronous and in a centrifugal way along

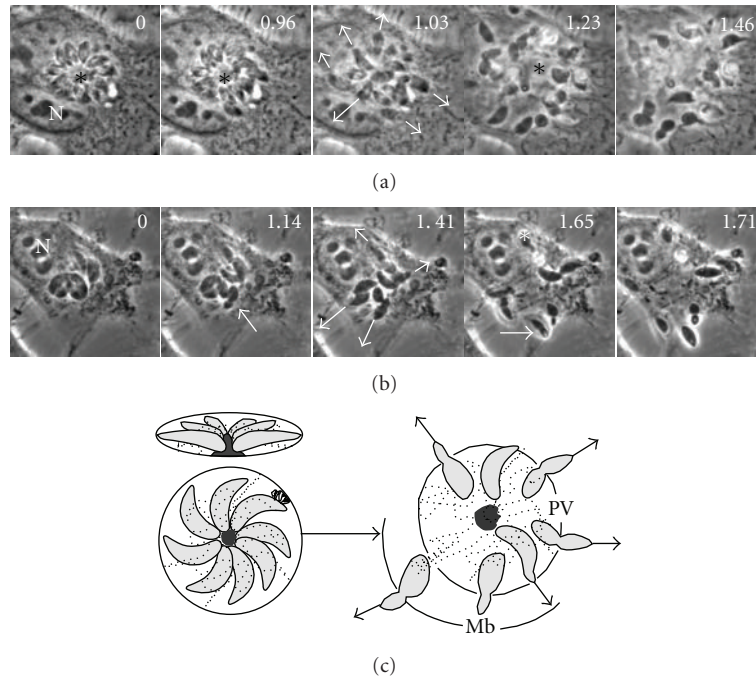


FIGURE 8: During exteriorization of tachyzoites, the residual body remains inside the PV. (a) Egress of RH tachyzoites arranged as “rosettes” from infected MDCK cells was induced by  $0.1 \mu\text{m}$  ionomycin and recorded by time lapse videomicroscopy. Externalizing parasites are indicated by the arrows. Arrowheads show the constriction of the tachyzoites passing through the host plasma membrane. The asterisk indicates remnants of the RB after the egress of parasites from a rosette. (b) The exteriorization of tachyzoites of  $\Delta\text{GRA}2$  strain was slightly slower than the RH strain. Several  $\Delta\text{GRA}2$  tachyzoites remained trapped in the cytoplasm or the nucleus (asterisks). Numbers in the upper right corners indicate the timing in seconds. N: nucleus of the host cell. Bars =  $5 \mu\text{m}$ . (c) represents the individual exteriorization routes followed by tachyzoites organized in rosettes.

individual routes to reach the extracellular medium as fast as  $1.3 \pm 0.5$  seconds (Figure 8(a), inset 1.03”, arrows). The trigger for the output started with a vibratory movement of the tachyzoites followed by twirling and sliding movements that were oriented to transverse the PVM followed by the plasma membrane. During externalization, there were two constrictions of the parasites, the first when they traversed the vacuolar membrane and the second when they passed through the cell membrane. The RB after the exteriorization remained inside the host cell (Figure 8(a), 1.23”, asterisk). The externalization of the  $\Delta\text{GRA}2$  strain was more erratic although very similar to the RH strain ( $1.6 \pm 0.7$  seconds). Although many parasites left the cell, several of them could not do it being trapped in the nucleus or the cytoplasm. Apparently, differences in egress time were not observed; however, one event important to remark is the fact that some parasites of  $\Delta\text{GRA}2$  mutant even if leave of parasitophorous vacuole are unable to leave their cells staying into of cytoplasm.

#### 4. Discussion

During the development of *Toxoplasma* within the PV, proteins secreted from dense granules contribute to the formation of new membranes, including those that form the PV and the MNN, but their function is poorly known in part due to the few experimental approaches available to isolate them and to gain access to the PV [1, 26].

Several technical procedures have been used to examine the intravacuolar arrangements of *Toxoplasma* including TEM analysis on thin sections and integration of serial optical sections obtained by confocal microscopy, although most of them have limitations in terms of image interpretation, resolution, or technical difficulty. One possibility to examine the inner structure of a cell and its organelles is by using the technique previously developed by Tanaka [18] and recently used in the study of *Toxoplasma* [15, 19]. In this method, the plasma membrane of cells previously processed for SEM is mechanically detached, exposing the spatial distribution of the intracellular organelles.

By applying the SEM technique in infected cells, we were able to study the arrangement of the intravacuolar tachyzoites in rosettes (Figure 1). According to our results, the rosette may represent a type of organization adopted by parasites to optimize the cytoplasmic space available for proliferation in cells with different phenotypes such as neurons, epithelial cells, muscle cells.

During endodiogeny, the favored type of tachyzoite division [27], the mother parasite forms two new dome-shaped conoids, each with an associated inner membrane complex and a set of microtubules and secretory organelles. Most of the mother cell cytoplasm and organelles are incorporated into the two daughter cells [28]. Although directly linked to the endodiogeny process, the RB is a structure that has been reported but poorly characterized; even more, it has been



suggested that the RB is degraded into the VP during posterior endodiogeny cycles [17]. The RB has also been considered as a product of stress condition, and it has been assumed that it is generated by treatments that affect an adequate assembly of the daughter cells. The RB is more easily observed when artificially enlarged as the result of ectopic protein expression or treatment with several drugs that affect the cytoskeleton [29, 30]. Presence of large RB (higher to  $5\ \mu\text{m}$ ) containing mitochondria and dense granules observed after exposure to actin-modifying drugs delayed or inhibited the parasite egress [31]. In parasites overexpressing myosin, the RB observed was lacking organelles or DNA [29].

In our study and under normal culture conditions and in absence of drugs, tachyzoites of RH strain proliferate around an RB to form intravacuolar rosettes. The RB is an interesting structure that has been considered as a waste material without a defined function [16, 29, 31, 32]. Here, we showed that it is a natural structure located in the centroid of the rosette. It was detected from the first cell division in PV containing two tachyzoites and appeared simultaneously to the formation of the MNN.

We consider that the RB may contain remnants released from the rear during cell division, but finding the parasites stably bound to it in the rosettes is very possible that the residual body fulfills a role as an organizer system in the rosette formation.

Although variations in the size of the RB were detected, there is no evidence to suggest that large or small residual bodies represent a defect in the process of endodiogeny.

The MNN has been considered as a tubule connection system between parasites and the PVM for exchange of nutrients and/or molecules between the host cell and the parasite [1]. The MNN consisted in tubules that keep connections between each daughter tachyzoites keeping them in close proximity to the PV [19]. Data obtained with RH and  $\Delta\text{GRA}2$  strains indicate that the MNN is an important structure involved in the maintenance of internal parasitic cohesion within the PV and that, somehow favors replicative cycle synchronization.

Absence of the GRA2 protein in the  $\Delta\text{GRA}2$  strain resulted in a complete loss of the MNN [14, 15] with the presence of atypical RBs.  $\Delta\text{GRA}2$  parasites organized in “clusters” instead of rosettes. GRA2 disruption resulted in the loss of parasite division synchrony, as observed by phase contrast microscopy in live cells and by SEM (Figures 6 and 7). These data suggest that the RB as well as the MNN favor the parasitic cohesion during the intravacuolar division and the parasitic arrangement in rosettes: the structural complex of MNN-RB and its extensions to the PVM would anchor the recently internalized parasites to the PVM to immobilize them as an initial necessary step to allow the synchronized proliferation of the parasites.

According to the SEM analysis in numerous samples, we proposed that formation of RB during organization of the rosette could involve the following steps (Figure 9); (I) a first parasite starts the endodiogeny process; (II) at the same time, MNN components are secreted through the posterior end of the parasite, followed by an apparent pinching event at the posterior end with a trapping of the pellicle and cytoplasm

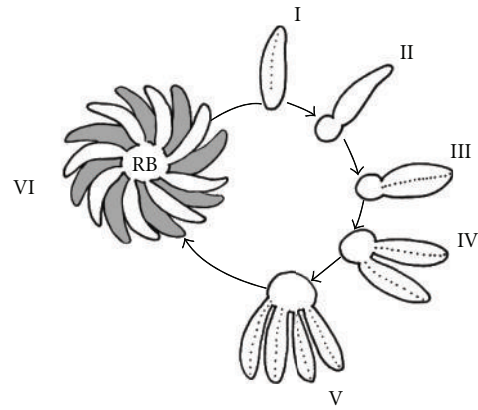


FIGURE 9: Formation of RB through of the endodiogeny process. (I) The first parasite into to PV; (II) during the early stages of the first division of the endodiogeny process, components are secreted and released toward the posterior end to form a first RB; (III) as tachyzoites proliferate, they release components to the posterior end and enrich the RB; (IV–VI) every new daughter remains attached to the RB starting the radial organization of the rosette.

components into a nascent RB that remains linked to the membrane of the posterior end of the parasite; (III–V) during the next replication cycles, the RB increases its size and the amount of stored material keeping all the time the daughter tachyzoites attached through their posterior end to the RB membrane. Maintenance of the interparasite space attached to the RB membrane determines the distribution of the parasites in a rosette organization (VI).

To date, there are no reports about the presence of RBs in infected animal tissues with *Toxoplasma*. Most reports about the intravacuolar organization of the parasite within infected animal tissues correspond to the presence of tissue cysts in animal models of toxoplasmosis. Of course, the study of the presence of RB's in the infected animal could be interesting and validate that our observations done *in vitro* are also occurring *in vivo*.

Although we studied the proliferation of tachyzoites in epithelial cells *in vitro*, under physiological conditions, tachyzoites or bradyzoites also come into contact with epithelial cells as enterocytes or endothelial cells from the vascular tissue, so it is possible that *in vivo Toxoplasma* can be organized in rosettes with a central RB.

## 5. Conclusions

Our study showed that (1) the RB is a spheroid structure occurring naturally during endodiogeny of RH strain (2) it is possible to observe this structure as soon as the first parasite division takes place, and it is formed simultaneously to the organization of the MNN; (3) it is limited by a membrane and it is probably formed from the first division by a pinching event of the posterior end membrane and through secretion of parasite's components; (4) during endodiogeny, daughter tachyzoites remain attached to the RB membrane showing a continuity between the RB and tachyzoites cytoplasm; (5) while the MNN determines interparasite cohesion, the RB

defines the spatial position in the rosette organization, acting like an organizing center during proliferating as a strategy to allow successful coordinated parasite division; (6) the RB may contain cytoplasmic organelles, such as mitochondria, nuclear fragments, and dense granules; (7) during exteriorization, the RB could determine the adequate parasite orientation with the aim to favor an efficient egress through individual routes of exteriorization; (8) the ability of exteriorization of the parasites attached to the RB indicates they are mature enough to display all the events involved in exteriorization, such as motility, conoid extrusion, and roptry secretion, and the RB does not represent an obstacle for such dynamic secretory processes; (9) interdigitated distribution in tachyzoites around the RB could optimize the intravacuolar space during proliferation; (10) lack of GRA2 protein produced atypical amorphous MNN and RB and absence of rosettes.

## Acknowledgments

Micrographs were obtained at the Electron Microscopy Unit, CINVESTAV, Mexico. Research was supported by CONACYT no. 155459 (to R. Mondragón). S. Muñoz-Hernández and M. González Del Carmen were supported by the doctoral fellowships no. 169932 and no. 176125 from CONACYT-Mexico, respectively.

## References

- [1] C. Mercier, K. D. Z. Adjogble, W. Däubener, and M. F. C. Delauw, "Dense granules: are they key organelles to help understand the parasitophorous vacuole of all apicomplexa parasites?" *International Journal for Parasitology*, vol. 35, no. 8, pp. 829–849, 2005.
- [2] V. Carruthers and J. C. Boothroyd, "Pulling together: an integrated model of *Toxoplasma* cell invasion," *Current Opinion in Microbiology*, vol. 10, no. 1, pp. 83–89, 2007.
- [3] A. J. Charron and L. D. Sibley, "Molecular partitioning during host cell penetration by *Toxoplasma gondii*," *Traffic*, vol. 5, no. 11, pp. 855–867, 2004.
- [4] D. G. Mordue, N. Desai, M. Dustin, and L. D. Sibley, "Invasion by *Toxoplasma gondii* establishes a moving junction that selectively excludes host cell plasma membrane proteins on the basis of their membrane anchoring," *Journal of Experimental Medicine*, vol. 190, no. 12, pp. 1783–1792, 1999.
- [5] I. Coppens, J. D. Dunn, J. D. Romano et al., "*Toxoplasma gondii* sequesters lysosomes from mammalian hosts in the vacuolar space," *Cell*, vol. 125, no. 2, pp. 261–274, 2006.
- [6] E. J. T. de Melo and W. de Souza, "A cytochemistry study of the inner membrane complex of the pellicle of tachyzoites of *Toxoplasma gondii*," *Parasitology Research*, vol. 83, no. 3, pp. 252–256, 1997.
- [7] A. P. Sinai and K. A. Joiner, "The *Toxoplasma gondii* protein ROP2 mediates host organelle association with the parasitophorous vacuole membrane," *Journal of Cell Biology*, vol. 154, no. 1, pp. 95–108, 2001.
- [8] A. P. Sinai, P. Webster, and K. A. Joiner, "Association of host cell endoplasmic reticulum and mitochondria with the *Toxoplasma gondii* parasitophorous vacuole membrane: a high affinity interaction," *Journal of Cell Science*, vol. 110, part 17, pp. 2117–2128, 1997.
- [9] J. F. Dubremetz, "Rhoptries are major players in *Toxoplasma gondii* invasion and host cell interaction," *Cellular Microbiology*, vol. 9, no. 4, pp. 841–848, 2007.
- [10] L. D. Sibley, I. R. Niesman, S. F. Parmley, and M. F. Cesbron-Delauw, "Regulated secretion of multi-lamellar vesicles leads to formation of a tubulovesicular network in host-cell vacuoles occupied by *Toxoplasma gondii*," *Journal of Cell Science*, vol. 108, part 4, pp. 1669–1677, 1995.
- [11] E. Labruyere, M. Lingnau, C. Mercier, and L. D. Sibley, "Differential membrane targeting of the secretory proteins GRA4 and GRA6 within the parasitophorous vacuole formed by *Toxoplasma gondii*," *Molecular and Biochemical Parasitology*, vol. 102, no. 2, pp. 311–324, 1999.
- [12] K. D. Z. Adjogble, C. Mercier, J. F. Dubremetz et al., "GRA9, a new *Toxoplasma gondii* dense granule protein associated with the intravacuolar network of tubular membranes," *International Journal for Parasitology*, vol. 34, no. 11, pp. 1255–1264, 2004.
- [13] L. Braun, L. Travier, S. Kieffer et al., "Purification of *Toxoplasma* dense granule proteins reveals that they are in complexes throughout the secretory pathway," *Molecular and Biochemical Parasitology*, vol. 157, no. 1, pp. 13–21, 2008.
- [14] C. Mercier, J. F. Dubremetz, B. Rauscher, L. Lecordier, L. D. Sibley, and M. F. Cesbron-Delauw, "Biogenesis of nanotubular network in *Toxoplasma parasitophorous vacuole* induced by parasite proteins," *Molecular Biology of the Cell*, vol. 13, no. 7, pp. 2397–2409, 2002.
- [15] L. Travier, R. Mondragon, J. F. Dubremetz et al., "Functional domains of the *Toxoplasma* GRA2 protein in the formation of the membranous nanotubular network of the parasitophorous vacuole," *International Journal for Parasitology*, vol. 38, no. 7, pp. 757–773, 2008.
- [16] K. Hu, T. Mann, B. Striepen, C. J. M. Beckers, D. S. Roos, and J. M. Murray, "Daughter cell assembly in the protozoan parasite *Toxoplasma gondii*," *Molecular Biology of the Cell*, vol. 13, no. 2, pp. 593–606, 2002.
- [17] E. van der Zypen and G. Piekarski, "Endodyogeny of *Toxoplasma gondii*—a morphologic analysis," *Zeitschrift für Parasitenkunde*, vol. 29, no. 1, pp. 15–35, 1967.
- [18] K. Tanaka, "High resolution scanning electron microscopy of the cell," *Biology of the Cell*, vol. 65, no. 2, pp. 89–98, 1989.
- [19] R. C. Magno, L. Lemgruber, R. C. Vommaro, W. de Souza, and M. Attias, "Intravacuolar network may act as a mechanical support for *Toxoplasma gondii* inside the parasitophorous vacuole," *Microscopy Research and Technique*, vol. 67, no. 1, pp. 45–52, 2005.
- [20] R. Mondragon, I. Meza, and E. Frixione, "Divalent cation and ATP dependent motility of *Toxoplasma gondii* tachyzoites after mild treatment with trypsin," *Journal of Eukaryotic Microbiology*, vol. 41, no. 4, pp. 330–337, 1994.
- [21] C. Rodriguez, D. Afchain, and A. Capron, "Major surface protein of *Toxoplasma gondii* (p30) contains an immunodominant region with repetitive epitopes," *European Journal of Immunology*, vol. 15, no. 7, pp. 747–749, 1985.
- [22] H. Charif, F. Darcy, G. Torpier, M. F. Cesbron-Delauw, and A. Capron, "*Toxoplasma gondii*: characterization and localization of antigens secreted from tachyzoites," *Experimental Parasitology*, vol. 71, no. 1, pp. 114–124, 1990.
- [23] A. Sadak, Z. Taghy, B. Fortier, and J. F. Dubremetz, "Characterization of a family of roptry proteins of *Toxoplasma gondii*," *Molecular and Biochemical Parasitology*, vol. 29, no. 2-3, pp. 203–211, 1988.
- [24] R. Mondragon and E. Frixione, "Ca<sup>2+</sup>-dependence of conoid extrusion in *Toxoplasma gondii* tachyzoites," *Journal of Eukaryotic Microbiology*, vol. 43, no. 2, pp. 120–127, 1996.

- [25] L. Lecordier, C. Mercier, L. D. Sibley, and M. F. Cesbron-Delauwz, "Transmembrane insertion of the *Toxoplasma gondii* GRA5 protein occurs after soluble secretion into the host cell," *Molecular Biology of the Cell*, vol. 10, no. 4, pp. 1277–1287, 1999.
- [26] M. F. Cesbron-Delauw, C. Gendrin, L. Travier, P. Ruffiot, and C. Mercier, "Apicomplexa in mammalian cells: trafficking to the parasitophorous vacuole," *Traffic*, vol. 9, no. 5, pp. 657–664, 2008.
- [27] F. Dzierszinski, M. Nishi, L. Ouko, and D. S. Roos, "Dynamics of *Toxoplasma gondii* differentiation," *Eukaryotic Cell*, vol. 3, no. 4, pp. 992–1003, 2004.
- [28] M. Nishi, K. Hu, J. M. Murray, and D. S. Roos, "Organelle dynamics during the cell cycle of *Toxoplasma gondii*," *Journal of Cell Science*, vol. 121, part 9, pp. 1559–1568, 2008.
- [29] F. Delbac, A. Sanger, E. M. Neuhaus et al., "Toxoplasma gondii myosins B/C: one gene, two tails, two localizations, and a role in parasite division," *Journal of Cell Biology*, vol. 155, no. 4, pp. 613–623, 2001.
- [30] X. Que, H. Ngo, J. Lawton et al., "The cathepsin B of *Toxoplasma gondii*, toxopain-1, is critical for parasite invasion and rhoptry protein processing," *Journal of Biological Chemistry*, vol. 277, no. 28, pp. 25791–25797, 2002.
- [31] M. K. Shaw, H. L. Compton, D. S. Roos, and L. G. Tilney, "Microtubules, but not actin filaments, drive daughter cell budding and cell division in *Toxoplasma gondii*," *Journal of Cell Science*, vol. 113, part 7, pp. 1241–1254, 2000.
- [32] Y. Wang, A. Karnataki, M. Parsons, L. M. Weiss, and A. Orlofsky, "3-Methyladenine blocks *Toxoplasma gondii* division prior to centrosome replication," *Molecular and Biochemical Parasitology*, vol. 173, no. 2, pp. 142–153, 2010.



**Hindawi**

Submit your manuscripts at  
<http://www.hindawi.com>

